Biodistribution and Radiation Dosimetry in Humans of a New PET Ligand, ^{18}F-PBR06, to Image Translocator Protein (18 kDa)

Yota Fujimura*, Yasuyuki Kimura*, Fabrice G. Siméon, Leah P. Dickstein, Victor W. Pike, Robert B. Innis, and Masahiro Fujita

Molecular Imaging Branch, National Institute of Mental Health, National Institutes of Health, Bethesda, Maryland

As a PET biomarker for inflammation, translocator protein (18 kDa) (TSPO) can be measured with an ^{18}F-labeled aryloxyanilide, ^{18}F-*N*-fluoroacetyl-*N*-(2,5-dimethoxybenzyl)-2-phenoxyaniline (^{18}F-PBR06), in the human brain. The objective of this study was to estimate the radiation absorbed doses of ^{18}F-PBR06 based on biodistribution data in humans. **Methods:** After the injection of ^{18}F-PBR06, images were acquired from head to thigh in 7 healthy humans. Urine was collected at various time points. Radiation absorbed doses were estimated by the MIRD scheme. **Results:** Moderate to high levels of radioactivity were observed in organs with high densities of TSPO and in organs of metabolism and excretion. Bone had low levels of radioactivity. The effective dose was 18.5 μSv/MBq. **Conclusion:** The effective dose of ^{18}F-PBR06, compared with other ^{18}F radioligands, was moderate. This radioligand had negligible defluorination, as indirectly assessed by bone radioactivity. Doses to the gallbladder wall and spleen may limit the amount of permissible injected radioactivity.

Key Words: MIRD scheme; defluorination; inflammation; microglia; aryloxyanilide

J Nucl Med 2010; 51:145–149
DOI: 10.2967/jnumed.109.068064

Translocator protein (18 kDa) (TSPO) is upregulated on activated microglia and macrophages and is, thus, a biomarker for inflammation (*1*). In the last several years, several improved PET ligands from new structural classes have been developed (*2–6*). We developed 2 aryloxyanilide-based ligands, ^{11}C-PBR28 (*7*) and ^{18}F-*N*-fluoroacetyl-*N*-(2,5-dimethoxybenzyl)-2-phenoxyaniline (^{18}F-PBR06) (*8*), both of which showed that approximately 90% of total activity was specific binding in the monkey brain (*9,10*). TSPO was well quantified in the human brain with both ^{11}C-PBR28 (*11*) and ^{18}F-PBR06 (*12*).

Received Jul. 8, 2009; revision accepted Sep. 25, 2009.
For correspondence or reprints contact: Masahiro Fujita, Molecular Imaging Branch, National Institute of Mental Health, Bldg. 31, Room B2B37, 31 Center Dr., MSC-2035, Bethesda, MD 20892-2035.
E-mail: fujitam@mail.nih.gov

*Contributed equally to this work.

^{18}F-labeled ligands provide better counting statistics than do ^{11}C-labeled ligands at late time points and allow distribution of the radioligand to distant institutions. However, potential concerns of ^{18}F-labeled ligands are an increase of radiation absorbed doses, which is due to the long half-life of ^{18}F, and accumulation of ^{18}F-fluoride ion, which is due to defluorination of the ligands and causes high bone activity spilling into adjacent organs in PET images.

The purposes of this study were to calculate the radiation absorbed doses of ^{18}F-PBR06; determine whether this radioligand is defluorinated, as indirectly assessed by bone uptake of radioactivity; and determine whether radiation doses to organs with high densities of TSPO will limit the amount of permissible injected activity.

MATERIALS AND METHODS

Radiopharmaceutical Preparation

^{18}F-PBR06 was synthesized by treating its bromomethyl analog with ^{18}F-fluoride ion and was purified with reversed-phase high-performance liquid chromatography, as described previously (*8*). The radioligand was prepared according to our Investigational New Drug application 23195 (*13*). Radiochemical purity was greater than 99% in all syntheses. Specific activity at the time of injection was 204 ± 50 GBq/μmol.

Human Subjects

Seven healthy volunteers (5 men and 2 women; mean age ± SD, 33 ± 11 y) participated in this study. On the basis of history, physical examination, electrocardiogram, urinalysis including drug screening, and blood tests (complete blood count, sodium, potassium, chloride, HCO_3, urea nitrogen, creatinine, glucose, calcium, phosphorus, alanine aminotransferase, aspartate aminotransferase, lactate dehydrogenase, alkaline phosphatase, creatine kinase, bilirubin, total protein, albumin, thyroid-stimulating hormone, and antibody screening for syphilis, HIV, and hepatitis B), all subjects were free of current medical and psychiatric illness. Our use of ^{18}F-PBR06 in human subjects was approved by the Radiation Safety Committee of the National Institutes of Health and the Institutional Review Board of the National Institute of Mental Health.

PET Scans

Subjects underwent ^{68}Ge transmission and dynamic emission scans using an Advance tomograph (GE Healthcare). After the injection of 185 ± 5 MBq of ^{18}F-PBR06, 2-dimensional dynamic PET scans were acquired for 300 min in 7 contiguous 15-cm bed positions from head to upper thigh in 16 frames. Each scan was of increasing duration in the following manner: first set of scans (a total of ~2 h, 1–116 min after injection: 4 frames of 15 s, 3 frames of 30 s, 3 frames of 1 min, 3 frames of 2 min, and 1 frame of 4 min); rest outside of camera; second set of scans (180–208 min after injection: 1 frame of 4 min); rest; and third set of scans (270–298 min after injection: 1 frame of 4 min). Blood pressure, pulse, respiration rate, and electrocardiogram were obtained before and at 15, 30, 90, 120, and 180 min after the injection.

Regions of interest were drawn on each coronal slice that visualized the source organs: brain, heart wall, lungs, spleen, liver, kidneys, gallbladder, and urinary bladder (Fig. 1). For each organ, we chose the most visible frame to draw the region and applied it to the remaining frames, with manual correction for motion. To estimate the residence time of bone and red marrow, regions were placed on the lumbar vertebrae, which contains both bone and red marrow, and on the ulna and radius, which contain only bone in adults (*14*). For the lumbar vertebrae, regions were drawn on summed sagittal slices to increase the contrast with surrounding tissue. For the bones in the forearm, which had low uptake of radioactivity, a single region was drawn over the ulna and radius on the transmission scan and then applied to the corresponding PET image. Image analysis was performed using PMOD, version 2.8 (PMOD Technologies).

Urine was collected from all subjects at about 120, 210, and 300 min after injection of the radioligand.

To study the pharmacologic effects of ^{18}F-PBR06, the blood and urine tests (except drug screening, syphilis, HIV, and hepatitis B) were repeated at approximately 24 h and approximately 1 mo after ^{18}F-PBR06 administration.

Residence Time Calculations

We used the organ activity that was corrected for the recovery of activity and the time points of the bed position in which the organ was primarily included. The area under the curve of each organ was calculated to the end of imaging by the trapezoidal method. The area after the last image to infinity was calculated by assuming only physical decay, without biologic clearance. The area under the curve of the fraction of measured injected activity from time zero to infinity is equivalent to the residence time.

Residence time of bone was estimated on the basis of that in the ulna and radius, which contain 4.3% of all bone mass in the body (*14*). The residence time of red marrow was estimated from the lumbar vertebrae. The bone and red marrow components of the lumbar vertebrae were 3.4% and 10.9%, respectively, of the total mass of each component in the body (*14*). Thus, the residence time of red marrow in the lumbar vertebrae was calculated as residence time of all lumbar vertebrae minus that in the bone component, which itself was calculated from the ulna and radius.

The residence time of the urinary bladder wall was calculated by applying the dynamic bladder model (*15*) to the combined data from images and urine samples. The decay-corrected cumulative activity in urine from all subjects was fit to a biexponential curve. The residence time was calculated on the basis of 2.4-h voiding intervals.

The residence times for all of the source organs were summed and subtracted from the fixed theoretic value of half-life/ln 2 = 2.64 h for ^{18}F to calculate the residence time of the remainder of the body for each subject.

Organ-Absorbed Dose

Radiation absorbed doses were calculated on the basis of the MIRD scheme by entering the average residence time of each source organ for 7 subjects into OLINDA 1.0/EXM software (*16*) for a 70-kg adult male.

Data are expressed as mean ± SD.

RESULTS

Pharmacologic Effects

The injected chemical dose of ^{18}F-PBR06 was 0.9 ± 0.2 pmol. On the basis of patient reports, electrocardiogram, blood pressure, pulse, and respiration rate, the dose caused no pharmacologic effects during the 5-h scan. Mean change of each of these parameters was less than 10%. In addition,

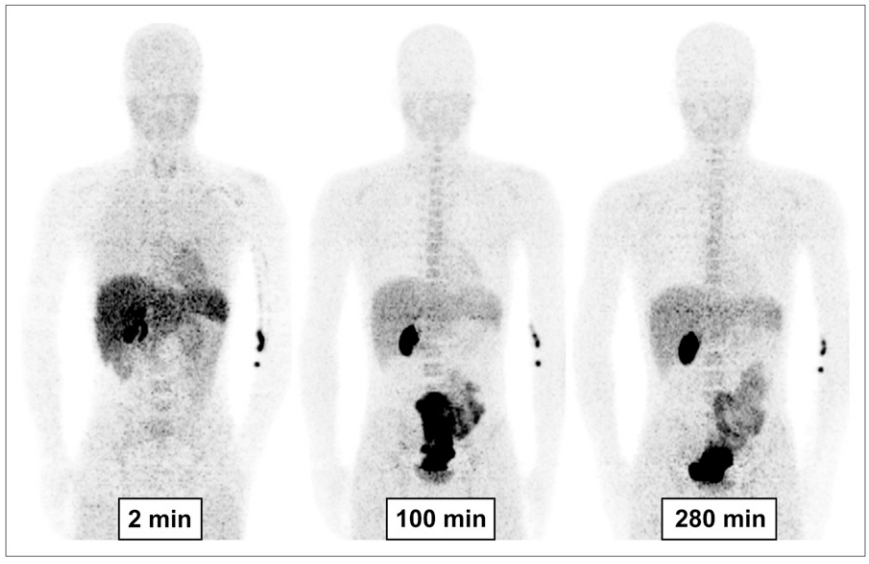

FIGURE 1. Biodistribution of radioactivity in healthy volunteer at about 2, 100, and 280 min after injection of ^{18}F-PBR06 (193 MBq). Images are decay-corrected and displayed using same gray scale. Although these maximum-intensity-projection images provide good visualization of organs, they are not quantitative and were not used to calculate radiation doses. First image was taken from 1 to 3 min with 15-s frames for each bed position. Second and third images were from 88 to 116 min and from 270 to 298 min, respectively, with 5-min frame for each bed position.

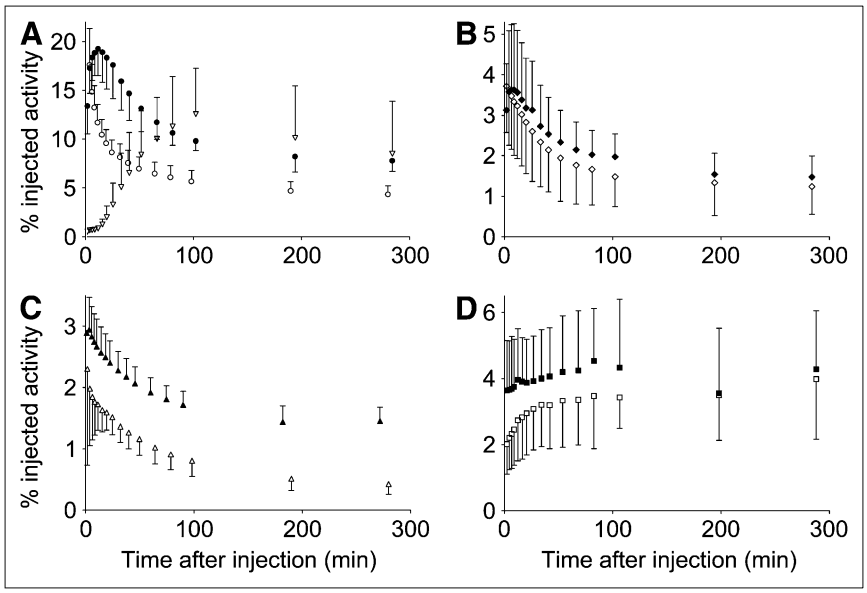

FIGURE 2. Time–activity curves of 7 source organs after injection of ^{18}F-PBR06. Decay-corrected data are average from 7 healthy subjects. Symbols represent mean, and error bars reflect SD. (A) Liver (●), lungs (○), and gallbladder (▽). (B) Spleen (◆) and kidneys (◇). (C) Brain (▲) and heart (△). (D) Red marrow (■) and bone (□). Activities in red marrow and bone were estimated from those in ulna and radius and in lumbar vertebrae. We deleted initial time point for lungs (24.6% ± 5.7% injected activity at 1.6 min) and error bar of initial time point for brain (1.4% injected activity at 1.0 min), because their high values unnecessarily extended *y*-axis.

no significant effects were noted in any of the blood and urine tests acquired about 24 h and 1 mo after radioligand injection.

Biodistribution

The distribution of radioactivity over time reflected blood volume, the relative densities of TSPO, and metabolism of the radioligand. For example, the lungs had the highest uptake (25% of injected activity) at early times (0–2 min), which largely reflected their high blood volume (Fig. 2A). The continued retention of moderate amounts of activity in the lungs reflected the high density of TSPO in these organs. Other organs with high densities of TSPO—including the kidneys, spleen, and heart wall—and the brain with low TSPO density were clearly visible and had high uptake and retention of radioactivity (Figs. 2B and 2C).

The metabolism of ^{18}F-PBR06 and excretion of radioactivity were predominantly via the hepatobiliary system and gastrointestinal tract. The high peak uptake in liver (19%) and gallbladder (13%) presumably reflected metabolism and excretion, respectively, via the gastrointestinal tract (Fig. 2A). The biexponential fitting of cumulative activity in urine indicated that 9.0% of injected activity was excreted via this route at infinite time, with biologic half-lives of 0.6 and 156 min (Fig. 3).

The estimated activity in all bones slowly accumulated and reached an asymptote of approximately 3.5% of injected activity within approximately 100 min (Fig. 2D). Compared with the activity in bone, that in all red marrow of the body was fairly constant during the scan and slightly higher (~3.9% of injected activity; Fig. 2D).

All subjects had a distribution of radioactivity that was expected from the known densities of TSPOs in the body. Thus, none of these subjects was a nonbinder, such as those we previously found with ^{11}C-PBR28 (*7*).

Organs of metabolism and excretion and those with high densities of TSPOs had the longest residence times (Table 1). Radiation absorbed doses (μSv/MBq) were highest in the gallbladder wall, spleen, and liver. The effective dose was 18.5 μSv/MBq (Table 2).

DISCUSSION

The effective dose of ^{18}F-PBR06 was 18.5 μSv/MBq, which was similar to that of many other ^{18}F-labeled radioligands. The doses to organs of metabolism (liver) and excretion (gallbladder) were relatively high and reflected the fact that the major excretory route of the radioactivity for this ligand is gastrointestinal. ^{18}F-PBR06

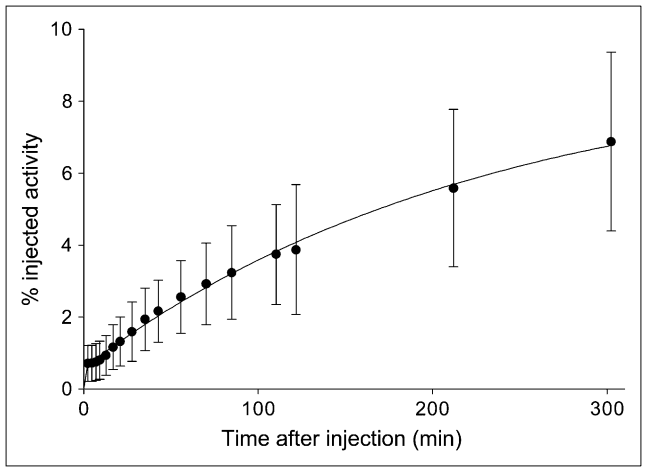

FIGURE 3. Cumulative urine activity measured from PET images and urine collection. Data derive from all subjects and are corrected for radioactive decay. Symbols represent mean, and error bars reflect SD. Solid line is biexponential curve and has asymptote of 9.0% of injected activity at infinite time and half-lives of 0.6 and 156 min.

TABLE 1. Residence Times of Source Organs and Remainder of Body Determined from 7 Healthy Subjects

Organ	Mean residence time (h) ± SD
Brain	0.05 ± 0.01
Liver	0.30 ± 0.03
Heart wall	0.02 ± 0.01
Lungs	0.18 ± 0.03
Red marrow	0.11 ± 0.04
Bone	0.09 ± 0.04
Gallbladder	0.22 ± 0.11
Kidneys	0.05 ± 0.02
Spleen	0.06 ± 0.02
Remainder of body	1.43 ± 0.13

was injected without any pharmacologic and toxic effect, as we expected, based on previous animal and human studies (*12,13*). Finally, bone had relatively little uptake, suggesting that ^{18}F-PBR06 undergoes little defluorination in vivo.

Effect of Organ Doses on Maximal Injected Activity

Limits of radiation exposure to research subjects vary within the United States and between countries, and there are 3 commonly used guidelines. First, radioactive drug research committees (RDRCs) operating in the United States under the auspices of the Food and Drug Administration have limits for both effective dose and individual organs, whichever occurs first (*17*). For ^{18}F-PBR06, the RDRC maximal activity would be 408 MBq based on the dose to the gallbladder wall, which has a maximal dose of 150 mSv. The guidelines at the National Institutes of Health for effective dose (http://drs.ors.od.nih.gov/services/rsc/forms_index.htm) give the maximal activity of 2.846 GBq based on the effective dose limit of 50 mSv per annum. Most countries in Europe allow a maximum dose that causes a minor-to-intermediate increase of risk and has a limit of 10 mSv (*18*). Thus, research subjects in Europe could receive no more 569 MBq of ^{18}F-PBR06 per annum. Because we have reported that injection activity of approximately 170 MBq allows accurate measurement of ^{18}F-PBR06 binding to TSPO in the brain (*12*), the radiation absorbed doses reported in the current study allow multiple scans under these guidelines.

Defluorination

We estimated the activity of all bones in the entire body based on the activity in the ulna and radius, which do not contain red marrow, and estimated the residence time of bone to be 0.09 h. This is only 8% of the residence time of bone after injection of ^{18}F-fluoride ion (1.12 h) (*19*). Therefore, ^{18}F-PBR06 showed low levels of defluorination, if any, in the human body. Vertebrae were dimly visible at late time points (Fig. 1) because, in addition to bone, they contain red marrow, which also showed a low level of residence time (0.11 h).

TABLE 2. Radiation Dose Estimates for ^{18}F-PBR06 Determined in 7 Healthy Subjects

Target organ	Radiation dose	
	μSv/MBq	mrem/mCi
Adrenals	16.0	59
Brain	10.0	37
Breasts	8.3	31
Gallbladder wall	367.0	1,360
Lower large intestine wall	10.5	39
Small intestine	13.3	49
Stomach wall	13.0	48
Upper large intestine wall	15.2	56
Heart wall	22.5	83
Kidneys	39.3	146
Liver	46.1	170
Lungs	36.5	135
Muscle	9.5	35
Ovaries	11.2	42
Pancreas	18.6	69
Red marrow	17.6	65
Osteogenic cells	21.6	80
Skin	6.8	25
Spleen	64.5	239
Testes	7.9	29
Thymus	10.0	37
Thyroid	8.5	31
Urinary bladder wall*	31.0	115
Uterus	11.9	44
Effective dose	18.5	69

*Determined from dynamic urinary bladder model with voiding interval of 2.4 h.

CONCLUSION

The effective dose of ^{18}F-PBR06 is moderate and similar to that of several other ^{18}F radioligands. ^{18}F-PBR06 undergoes low levels of defluorination in humans. Depending on local guidelines for radiation exposure to research subjects, the relatively high dose to the gallbladder may limit the amount of injected radioactivity.

ACKNOWLEDGMENTS

We thank Maria D. Ferraris Araneta, Barbara A. Scepura, and Gerald L. Hodges for screening and care of the subjects; the staff of the PET Department for successful completion of PET scans; the staff of the Clinical Center for ^{18}F production; Jeih-San Liow and Robert L. Gladding for assisting with data processing; and PMOD Technologies (Zurich, Switzerland) for providing its image-analysis and modeling software. This research was supported by the Intramural Program of the NIMH-NIH (project Z01-MH-002852-04) and by a JSPS Research Fellowship in Biomedical and Behavioral Research at NIH.

REFERENCES

1. Zisterer DM, Williams DC. Peripheral-type benzodiazepine receptors. *Gen Pharmacol.* 1997;29:305–314.

2. Chauveau F, Boutin H, Van Camp N, Dollé F, Tavitian B. Nuclear imaging of neuroinflammation: a comprehensive review of [^{11}C]PK11195 challengers. *Eur J Nucl Med Mol Imaging.* 2008;35:2304–2319.
3. Chauveau F, Van Camp N, Dolle F, et al. Comparative evaluation of the translocator protein radioligands ^{11}C-DPA-713, ^{18}F-DPA-714, and ^{11}C-PK11195 in a rat model of acute neuroinflammation. *J Nucl Med.* 2009;50:468–476.
4. Fookes CJ, Pham TQ, Mattner F, et al. Synthesis and biological evaluation of substituted [^{18}F]imidazo[1,2-*a*]pyridines and [^{18}F]pyrazolo[1,5-*a*]pyrimidines for the study of the peripheral benzodiazepine receptor using positron emission tomography. *J Med Chem.* 2008;51:3700–3712.
5. Wang M, Gao M, Hutchins GD, Zheng QH. Synthesis of [^{11}C]FEDAA1106 as a new PET imaging probe of peripheral benzodiazepine receptor expression. *Eur J Med Chem.* 2009;44:2748–2753.
6. Yasuno F, Ota M, Kosaka J, et al. Increased binding of peripheral benzodiazepine receptor in Alzheimer's disease measured by positron emission tomography with [^{11}C]DAA1106. *Biol Psychiatry.* 2008;64:835–841.
7. Briard E, Zoghbi SS, Imaizumi M, et al. Synthesis and evaluation in monkey of two sensitive ^{11}C-labeled aryloxyanilide ligands for imaging brain peripheral benzodiazepine receptors in vivo. *J Med Chem.* 2008;51:17–30.
8. Briard E, Zoghbi SS, Siméon FG, et al. Single-step high-yield radiosynthesis and evaluation of a sensitive ^{18}F-labeled ligand for imaging brain peripheral benzodiazepine receptors with PET. *J Med Chem.* 2009;52:688–699.
9. Imaizumi M, Briard E, Zoghbi SS, et al. Brain and whole-body imaging in nonhuman primates of [^{11}C]PBR28, a promising PET radioligand for peripheral benzodiazepine receptors. *Neuroimage.* 2008;39:1289–1298.
10. Imaizumi M, Briard E, Zoghbi SS, et al. Kinetic evaluation in nonhuman primates of two new PET ligands for peripheral benzodiazepine receptors in brain. *Synapse.* 2007;61:595–605.
11. Fujita M, Imaizumi M, Zoghbi SS, et al. Kinetic analysis in healthy humans of a novel positron emission tomography radioligand to image the peripheral benzodiazepine receptor, a potential biomarker for inflammation. *Neuroimage.* 2008;40:43–52.
12. Fujimura Y, Zoghbi SS, Siméon FG, et al. Quantification of translocator protein (18 kDa) in the human brain with PET and a novel radioligand, ^{18}F-PBR06. *J Nucl Med.* 2009;50:1047–1053.
13. NIMH/SNIDD Tracer Database Initiative. Complete IND and FDA review, PET imaging of peripheral benzodiazepine receptors with [^{18}F]FBR. Available at: http://pdsp.med.unc.edu/snidd/IND/PBR06.php. Accessed August 21, 2009.
14. The International Commission on Radiological Protection. Report of the task group on reference man. ICRP Publication 23. Tarrytown, NY: Pergamon Press; 1975.
15. Cloutier RJ, Smith SA, Watson EE, Snyder WS, Warner GG. Dose to the fetus from radionuclides in the bladder. *Health Phys.* 1973;25:147–161.
16. Stabin MG, Sparks RB, Crowe E. OLINDA/EXM: the second-generation personal computer software for internal dose assessment in nuclear medicine. *J Nucl Med.* 2005;46:1023–1027.
17. Prescription drugs for human use generally recognized as safe and effective and not misbranded: drugs used in research, 21 CFR §361.1 (2008).
18. The International Commission on Radiological Protection. Radiological protection in biomedical research. ICRP Publication 62. Tarrytown, NY: Pergamon Press; 1993.
19. The International Commission on Radiological Protection. Radiation dose to patients from radiopharmaceuticals. ICRP Publication 53. Maryland Heights, MO: Elsevier; 1988.